Journal of the Physical Society of Japan
Vol. 78, No. 3, March, 2009, 034402
©2009 The Physical Society of Japan

Crack-Tip Stress Concentration and Structure Size in Nonlinear Structured Materials

Yuko AOYANAGI and Ko OKUMURA*

Department of Physics, Graduate School of Humanities and Sciences, Ochanomizu University, 2-1-1 Otsuka, Bunkyo-ku, Tokyo 112-8610

(Received September 24, 2008; accepted December 25, 2008; published March 10, 2009)

We revisit the standard elastic-plastic fracture theory developed by Hutchinson, Rice, and Rosengren (HRR) and reproduce, by a simple scaling argument, the stress singularity around the crack tip derived by HRR. From the singular behavior thus reconfirmed, we propose a general scaling relation which guarantees an effect similar to the tip-blunting effect: the maximum stress at the crack tip in a structured material can be reduced by increasing the structure size. This proposed relation is explicitly confirmed by numerical calculations performed for a coarse-grained lattice model, and leads to general scaling relations for fracture surface energy and to a possible reinforcement of cellular solids due to the pores.

KEYWORDS: fracture mechanics, fracture surface energy, scaling laws, soft matter physics, adhesion
DOI: 10.1143/JPSJ.78.034402

1. Introduction

A widespread strategy to fulfill the quest for stronger materials is to exploit composite structures, from simple foam to modern carbon nanotube composites,[1] sometimes mimicking natural strong materials[2,3] such as nacre[4,5] and bone.[6] In the case of cellular solids[7] which include wood, cork, plant parenchyma, stereom of sea cucumber, trabecular bone, carbon and polymeric foams and porous materials, theories based on the unit cell structure have been successful to reveal that fracture mechanical properties can be well understood as a function of the relative density (i.e., volume fraction of solid in foam) in particular for hard cellular solids;[7,8] this is confirmed recently even for very soft foams but with different scaling relations.[9] Further progress has been propelled through more inclusion of detailed structures into theory such as imperfection and randomness, which leads to computational modeling based on finite-element method.[10,11] Similar trend prevails in most of modern theoretical treatments of high performance composites, for example, nacre,[12] bone,[13] and carbon nanotube composite.[14] This spirit differentiates theories seeking results specific to a certain material.

However, all of these composites have a feature in common: at macroscopic level it follows a non-linear stress–strain relation at least near critical of failure and this macroscopic continuum view breaks down on a cut-off scale due to internal inhomogeneous structures. Note that at large strains most macroscopic stress–strain relations can be approximated by a non-linear relation (e.g., a nonlinear elastic model can describe a form of plasticity, known as "deformation plasticity", provided no unloading occurs[15]). In this paper, we examine what we can deduce from this common feature with the expectation that the results thus obtained can be universally applicable to various composites or structured materials.

We focus in particular on *the crack-tip stress* where local stress is maximally enhanced: strength of materials is measured by the failure stress at which materials start to break when extended; they begin to fail from a small flaw or crack because the local stress at the crack tip is enhanced from the remote stress.[16] Reduction of such crack tip stress, by minimizing size of flaws[17] or by exploiting a laminar structure,[18] could be a way to reinforce materials. We could reinforce materials also by embedding spherical voids (or particles) in materials,[19] because a sharp crack is stopped when it meets such a cavity: it is well-known that the crack tip is blunted by the void.[15] However, in materials with many voids or in structured materials, including cellular solids, porous materials, foams and gels, the continuum view breaks down on the scale of cell size. In such a situation, precise scaling relations among the crack tip stress, the failure stress and characteristic size of voids or of an internal structure are unknown. Here, we derive simple and universal relations among them in a typical elastic-plastic model[20,21] and confirm the relations in a grid model by numerical calculations. The results lead to general scaling relations for fracture energy and to a possible toughening mechanism of cellular solids due to the voids.

This paper is organized as follows: (1) firstly, we develop scaling arguments to propose some relations, which motivated the present work, (2) secondly, we construct a lattice model and show the results of numerical calculations to check our proposals, and (3) finally, based on the relations we derive scaling relations for fracture energy to conclude a possible reinforcement mechanism for cellular solids.

2. Scaling Arguments

Relation between stress σ and strain ε in most materials at large strains can be cast into the form,

$$\sigma = \mu \varepsilon^{1/n} \tag{1}$$

with fixed n: $n = 1$ corresponds to linear elastic materials and $n > 1$ to elastic-plastic materials for nearly yielded regime. Throughout this article, we ignore numerical coefficients and tensorial properties of stress and strain but clarify scaling relations between characteristic sizes of important physical quantities.

Note that the strain-stress relation in eq. (1) is nothing but a simple nonlinear elastic model but can describe a form of plasticity, known as "deformation plasticity", provided no unloading occurs. Accordingly, we develop the following

*E-mail: okumura@phys.ocha.ac.jp

scaling arguments as if we were dealing with a nonlinear elastic model: our discussions and conclusions below can be regarded for a simple nonlinear material but can be useful also for a certain form of elastic-plastic materials.

Consider an infinite plate of a material governed by eq. (1) at large strains with a line crack of size a, under a remote tensile stress σ_0 applied in the direction perpendicular to the line crack, and examine the energy balance per unit thickness of the plate at the critical of failure, following the Griffith's idea.[17,22] The energy (per unit thickness) required to create the crack of length a scales as γa. Here, γ is the fracture surface energy per unit area, which is often dominated by a plastic contribution. A characteristic nonlinear elastic energy per unit volume scales as $\sigma_0\varepsilon$. Due to the existence of the crack, nonlinear elastic energy should be reduced in total. The amount of reduction scales as the nonlinear elastic energy, localized in a volume of the order of a^2 (per unit thickness), because the only length scale available in this problem is the crack length a. When this energy gain $\sigma_0\varepsilon a^2$ is balanced with the energy loss γa, we obtain a generalized Griffith law:

$$\sigma_{\mathrm{F}} \sim (\mu^n\gamma/a)^{1/(n+1)} \tag{2}$$

at the critical of failure. Here, σ_{F} is the failure stress, i.e., the critical value of σ_0. Equation (2) reduces to the well-known Griffith's criteria for the linear-elastic fracture mechanics at $n = 1$.

Separately from the above argument, stress distribution $\sigma(r)$ in this material as a function of distance r from the crack tip should be described by the following form $\sigma(r) = \sigma_0(a/r)^{\delta}$ near the tip with an unknown exponent δ because σ recovers to σ_0 at $r \sim a$, considering all the dimensional quantities available for this expression. Now, we require that $\sigma(r)$ near the tip be independent of a at the critical of failure, after replacing σ_0 by σ_{F} given in eq. (2), because we are interested in the limit, $r \ll a$. This requirement determines the exponent δ to be $1/(n+1)$ and leads to the relation,

$$\sigma(r)/\sigma_0 \sim (a/r)^{1/(n+1)} \quad (r \ll a) \tag{3}$$

This relation, reproduced by a simple scaling argument, coincides with the HRR singularity.[20,21]

This expression diverges at the tip ($r \sim 0$), which suggests a cut off in real materials. Accordingly, in a material with many voids or with an internal structure whose largest characteristic size d, the maximum stress σ_{M} which appears at the tip may scale as

$$\sigma_{\mathrm{M}}/\sigma_0 \simeq (a/d)^{1/(n+1)} \quad (d \ll a) \tag{4}$$

because the continuum model breaks down on scales smaller than d. This predicts how the maximum stress at the crack tip is enhanced from the remote stress depending on the void size d: the crack-tip stress gets reduced as the structure size increases. This effect might remind us the well-known tip-blunting effect.[15]

3. Numerical Simulations

Equation (4) can be directly checked by numerical calculations. In our simulation, a structure with voids or with an internal structure is described by *a two-dimensional lattice model* (Fig. 1) composed of $N \times N$ points, initially arranged in a two dimensional square lattice, with each point $\mathbf{X}_{ij}$ connected to the four nearest neighbors $\mathbf{X}_{ij}^{(s)}$,

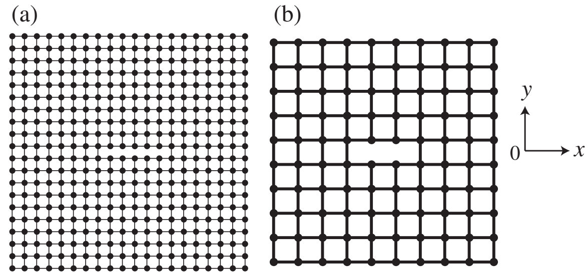

Fig. 1. The illustration of coarse-grained grid models with different mesh sizes, with a crack in the middle, to be stretched in the y direction, governed by eq. (1). Here, the crack size a and the system size L (when N is large) are the same for both systems, but the mesh size is doubled in (b). A thick spring in (b) is composed of four thin springs in (a) so that the total numbers of thin springs in (a) and (b) are the same when N is large (in order to have the same macroscopic property).

$$\mathbf{X}_{ij}^{(s)} = \begin{cases} \mathbf{X}_{i+1\,j} & (s=1) \\ \mathbf{X}_{i\,j+1} & (s=2) \\ \mathbf{X}_{i-1\,j} & (s=3) \\ \mathbf{X}_{i\,j-1} & (s=4) \end{cases} \tag{5}$$

with a nonlinear spring of natural length l. The four springs attached to a point (i, j) provide force reflecting eq. (1) whose α (x or y) component is given by

$$F_{i,j,\alpha} = \sum_{i,j=1}^{N}\sum_{s=1}^{4} k(i,j,s)(\mathbf{X}_{i,j}^{(s)} - \mathbf{X}_{i,j} - \boldsymbol{l}^{(s)})_{\alpha}^{1/n} \tag{6}$$

where

$$\boldsymbol{l}^{(s)} = \begin{cases} (l,0) & (s=1) \\ (0,l) & (s=2) \\ (-l,0) & (s=3) \\ (0,-l) & (s=4) \end{cases} \tag{7}$$

The nonlinear spring constant $k(i, j, s)$ is set to a constant k everywhere except at the boundary (i.e., i or/and j are either 1 or N).

A similar but different model composed of quasi linear springs is discussed in[23] where the exponent n in eq. (4) is close to one but weakly dependent on the strain due to a weak nonlinearity. In our model, compared with this previous model, due to the absence of coupling between the x and y components of $\mathbf{X}_{i,j}$ vectors, the inter-distance between the adjacent points $\mathbf{X}_{i,j}$ in the x direction is always fixed to d, which might seem to be an oversimplification but has a strong advantage that the smallest length scale in x direction, i.e., the cut-off length, is kept fixed; in the previous model, since the inter-distance (i.e., the cut-off length) can change in response to external force due to the coupling, unwanted ambiguity on the definition of the cut-off length scale was introduced, which makes the analysis delicate.

To confirm eq. (4) we magnify the mesh size d_m from l to ml so that the new system is composed of $N/m \times N/m$ points where the new system size $L_m = ml(N/m - 1) \simeq Nl$ is independent of m for large N. For convenience, we make the bulk elastoplastic property also independent of m; this would be accomplished intuitively and is checked explicitly below if we use the same ingredients to make systems of the same size L so that we require that a spring in the new system is constructed as m bundles of m serial connections of the original spring: the total number of original spring contained in the network become the same for the two systems in the large N limit (see Fig. 1).

When a new spring thus composed is stretched by Δx (i.e., each original spring by $\Delta x/m$), the total force F applied at the both ends is summed up to $mk(\Delta x/m)^{1/n}$: the new spring constant is

$$k_m = m^{1-1/n}k \tag{8}$$

This states that two-dimensional stress defined as $\sigma \equiv F/ml$ (since a new spring supports an area ml) scales as $\sigma = k_m(\varepsilon ml)^{1/n}/ml$ for strain ε, which is independent of m, i.e., $\sigma = \mu\varepsilon^{1/n}$ with $\mu = kl^{1/(n-1)}$. This argument confirms that magnification of mesh size without changing the bulk elastoplastic property is realized in this scheme. In addition, if we imagine that the shape of original springs are a cylinder of the same radius the volume fraction of spring (i.e., solid fraction in foam) is always the same irrespective of m: this clearly demonstrates that in cellular solids the bulk response is unchanged if the relative density is fixed.

From this prescription of mesh magnification, we can generalize eq. (6) into the form,

$$\sigma^{(m)}_{i,j,\alpha} = \frac{1}{2}\sum_{i,j=1}^{N}\sum_{s=1}^{4}\mu(i,j,s)(\overline{\mathbf{X}}^{(s)}_{i,j} - \overline{\mathbf{X}}_{i,j} - \overline{\boldsymbol{l}}^{(s)})^{1/n}_{\alpha} \tag{9}$$

where $\sigma^{(m)}_{i,j,\alpha} = F^{(m)}_{i,j,\alpha}/ml$, $\mu(i,j,s) = k(i,j,s)l^{1/(n-1)}$, $\overline{\mathbf{X}} = \mathbf{X}/ml$, and $\overline{\boldsymbol{l}}^{(s)} = \boldsymbol{l}^{(s)}/l$. Here, $F^{(m)}_{i,j,\alpha}$ is defined by eq. (6) with $\boldsymbol{l}^{(s)}, k$ replaced by $m\boldsymbol{l}^{(s)}, k_m$, respectively.

A pseudo line crack is introduced into the network by cutting n_a bonds in the middle ($y = 0$), i.e., by setting $k(i,j,s)$ to zero at corresponding points ($j = N/2$ for $s = 2$ and $j = N/2+1$ for $s = 4$ for even N). Here, the crack length a and the void size d are identified with $(n_a+1)ml$ and ml, respectively.

The network with the crack thus introduced is stretched in the y direction so that the strains at upper and lower ends, initially located at $y = \pm L/2$, are $\pm\varepsilon$, and the equilibrium force distribution is obtained via numerical calculations by solving a coupled equations of motions,

$$\eta\frac{\mathrm{d}X_{ij\,\alpha}}{\mathrm{d}t} = F^{(m)}_{i,j,\alpha} \tag{10}$$

The dynamics can be relaxed to a unique equilibrium state, after a sufficient time t. The damping constant η changes only the dynamical process to reach the equilibrium state: results obtained below are insensitive to η.

Numerical scheme explained above is performed for various mesh size $d_m = ml$, crack size a, and remote strain ε, at a given exponent n. We confirmed that calculated force distribution at the relaxed states always shows the maximum F_{M} at the crack tip as expected. With use of F_{M} thus obtained, we calculate σ_{M} which (normalized by $\sigma_0 \equiv \mu\varepsilon^{1/n}$) are plotted as a function of a/d at $n = 1$ and $\varepsilon = 1.5$ in Fig. 2, where eq. (4) is confirmed for various a, and d.

To obtain a precise exponent, we note two conditions required for comparison of our simulation in a *finite* system with eq. (4) derived in an *infinite* system: one for the system size, $L \gg a$, and the other for a line crack or for the scaling behavior, $a \gg d$: for $L \gg a$ we fix the system size $L = Nl$ to a large size $400l$ (in all calculations, d_m and a are less than $5l$ and $40l$, respectively), and for $a \gg d$ we used only first two left points ($m = 1$ and 2) for a given a to determine the slope of the line fitting the data. The three slopes thus obtained by using the data in Fig. 2 slightly depends on the crack size a (but the differences are less than 0.5 per cent) and the slope for $a = 20l$ gives a slope closest to the theoretical value, $-1/2$; $a = 10l$ is the best for $L \gg a$ while $a = 40l$ is the best for $a \gg d$: $a = 20l$ is the best in total, which is the reason why we use the crack size $a = 20l$ below to determine exponents by simulation.

Exponents ν in relation $\sigma_{\mathrm{M}}/\sigma_0 \simeq (d/a)^{-\nu}$ for various n in eq. (1) are extracted as the slope of each line in Fig. 3, where from the above reason the first two left points in each series in Fig. 3 are used to determine the slope; the results are summarized in Table I, where the relation $\nu = 1/(n+1)$ holds for every pair; this again confirms eq. (4) for various n.

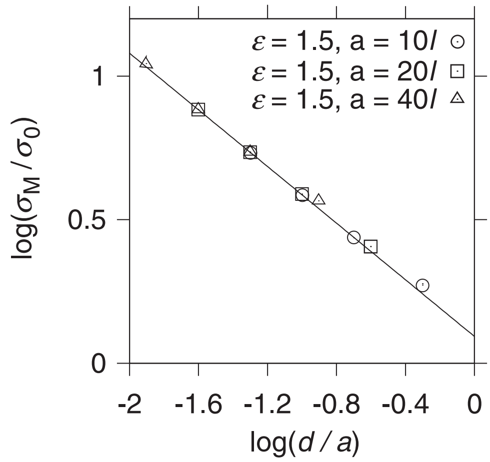

Fig. 2. Confirmation of eq. (4) at $n = 1$ and $\varepsilon = 1.5$ for various a and d: the maximum stress which appears in the network becomes smaller as the mesh size gets larger. The solid line shows the slope $-1/(n+1) = -1/2$ expected in the limits, $L \gg a$ and $a \gg d$.

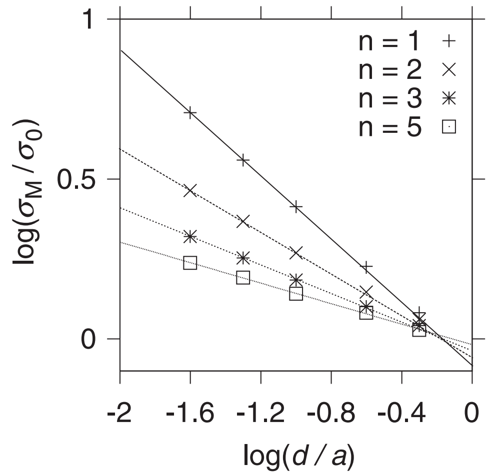

Fig. 3. Relation between $\sigma_{\mathrm{M}}/\sigma_0$ and d/a for various n at $\varepsilon = 1.5$ and $a = 20l$. The solid lines fit the two leftmost points in each series.

Table I. The exponent ν determined from Fig. 3.

n	1	2	3	5
ν	0.50	0.33	0.25	0.16

4. Discussion

We obtain important scaling relations from eqs. (2) and (4), in the latter of which the maximum stress $\sigma_{\rm M}$ at the critical of failure is identified with yield stress when plastic deformation occurs at the tip. At this critical of failure eq. (4) reads as

$$\sigma_{\rm F}/\sigma_{\rm Y} \simeq (d/a)^{1/(n+1)} \quad (d \ll a) \tag{11}$$

Here, $\sigma_{\rm Y}$ is the yield stress, i.e., the maximum or tip stress $\sigma_{\rm M}$ at the critical of failure, which is unique to a material in question. From eqs. (2) and (11) we obtain

$$\gamma \sim \sigma_{\rm Y}^{n+1} d/\mu^n \tag{12}$$

Physical interpretation of this relation becomes transparent if we rewrite this by introducing a yield strain $\varepsilon_{\rm Y}$ defined as $\sigma_{\rm Y} \sim \mu \varepsilon_{\rm Y}^{1/n}$ into the form

$$\gamma \sim \sigma_{\rm Y} \delta \tag{13}$$

with a displacement δ

$$\delta \sim \varepsilon_{\rm Y} d \tag{14}$$

Equation (13) implies that the fracture energy scales as the work per unit area to deform a cell at the crack tip by displacement δ under the yield stress $\sigma_{\rm Y}$, i.e., the work to cause "plastic" deformation at the tip; δ can be interpreted as the crack-tip opening distance.[15] When the yielded region is smaller in scale than the structure size d where our Griffith-type failure criteria is allowed probably due to the Irwin–Orowan-type extension,[24,25] we expect that δ is independent of d as opposed to the formal definition in eq. (14) because plastic deformation is localized in the scale smaller than d: criteria of the plastic failure is determined by the process localized at the yielded region. As a matter of fact, we confirmed, together with this independence of δ on d, eqs. (4), (12), and (13) directly in experimental studies on non-crosslinked polyethylene foam,[9] which will be discussed elsewhere.

For cellular solids with different mesh sizes d, (A) the yield stress $\sigma_{\rm Y}$ can be the same if the volume fraction is fixed and (B) a fixed volume fraction can be identical to a fixed bulk elasticity. The statement (A) can be understood as follows. The yield stress $\sigma_{\rm Y}$ of cellular solids made from the same material is a function of the volume fraction ϕ of solid: $\sigma_{\rm Y} = \phi \sigma_{\rm Y}^{(s)}$ where $\sigma_{\rm Y}^{(s)}$ is the yield stress of the solid ($\phi = 1$). This is because the volume fraction can be identified with area fraction in cellular solids as demonstrated in ref. 9. This means that $\sigma_{\rm Y}$ is unchanged even if the cell size d is varied, if the volume fraction ϕ is kept fixed. This can be understood also by reminding the discussion on the grid model given around eq. (8); as discussed above, if we construct several two-dimensional networks, of the same size but of different mesh sizes $d = ml$, by using the same number of original "cylindrical" springs of the same radius, the volume fraction of the networks thus constructed are the same; if we assume that each original spring tears off at the same critical force $f_{\rm Y}$, the (two-dimensional) yield stress $\sigma_{\rm Y}$ of the networks in question are the same because there are m original springs per one mesh ($\sigma_{\rm Y} = mf_{\rm Y}/ml$); in other words, if the volume fraction is the same, the yield stress is the same for these networks. The statement (B) can be understood as follows. In certain cellular solids the "elastic modulus" is also determined by ϕ (as demonstrated in the linear-elastic case in ref. 9: $\mu = \phi \mu_{\rm s}$ where $\mu_{\rm s}$ is the modulus of the solid). This is clearly the case of the two-dimensional network model as discussed in the above: we can make the bulk elasticity the same if we use the same number of original springs to make networks of the same size (i.e., if the volume fraction is the same).

From (A) and (B), we see that (C) $\sigma_{\rm Y}$ is unchanged even if the cell size d is varied, if the bulk elasticity is kept fixed. The statement (C) together with eq. (11) suggests that, in cellular solids, if the volume fraction or the bulk elasticity is fixed, the stress concentration can be reduced by increasing the mesh size: strength of cellular solids under the existence of a macroscopic crack can be enhanced by increasing the mesh size. However, this statement should be interpreted with care; the strength of cellular solids made from the same material can be reduced with increase in the mesh size in reality if the volume fraction is not fixed, as will be discussed in a separate experimental study.

Although our result is quite general, derived only from assumptions of nonlinear stress–strain relation at large strains and a cut-off scale for the relation, there are some practical limitations associated with requirements in the derivation. Firstly, we require the existence of a macroscopic crack of size a larger than d: eqs. (4) and (11) cannot predict the inherent strength when macroscopic crack is absent. In such a case, randomness and imperfection become important issues but these effects are "averaged out" for the strength under the existence of a macroscopic crack. Secondly, in deriving a conclusion on the strength enhancement in cellular solids, we require that systems with deferent d should look in the same way on a scale larger than d. This requirement is fulfilled by keeping the same ratio of ingredients to make materials of the same bulk size but with different structure size in many cases, as explicitly demonstrated in the lattice model. In cellular solids, this corresponds to fix the volume fraction of solids (i.e., the relative density) but to change the cell size. This inevitably allows us to explore the region outside the scope of previous studies of cellular solids where properties are mainly understood as a function of the relative density. However, in practical development of new materials, it would be sometimes difficult to find a way to change largest structure size without changing bulk properties.

As indicated before, our grid model lacks the coupling between the x and y components of $\mathbf{X}_{i,j}$ vectors: our system is free from shear stress. Considering this point, our confirmation of eq. (4) by numerical calculation is limited and for completeness it would be important to confirm eq. (4) in a more realistic model, for example, in a square-lattice model but with extra diagonal springs or in a triangular-lattice model, where shear stress comes into play. However, we will study this point in a separate paper, because (1) as mentioned before, this introduces some ambiguity on the definition of "mesh size" since local mesh size around the crack tip is strongly changed from the original size due to shear, which needs a careful treatment, and (2) despite of this difficulty we have confirmed already eq. (4) for $n = 1$ (linear case) in a numerical model which does include the effect of shear in ref. 23 so that we can expect to some extent that our numerical results for nonlinear cases may be unchanged even if we introduce the effect of shear deformation.

5. Conclusion

In conclusion, (A) we reproduce the HRR singularity at the crack tip of elastic-plastic materials in eq. (3) by a simple argument, (B) propose relations between measures of fracture strength and cut-off scale in eq. (4) based on eq. (3), (C) confirm this by numerical calculations, and (D) derive scaling laws for fracture energy in eqs. (12) and (13) from eqs. (3) and (4). The proposed relations thus established in this study implies that *under a fixed volume fraction or a bulk elasticity, increase in void or structure size can lead to reinforcement of the structured material*. Note that the void or structure size is always restricted from the above, in practical situations; e.g., the maximum mesh size of a net for filtering is determined by the size of particles to be filtered.

Acknowledgments

K.O. is grateful to Satoko Nakagawa for her help in the early stage of this work. K.O. thanks the Ministry of Education, Culture, Sports, Science and Technology, Japan, for a Grant-in-Aid for Scientific Research.

1) P. J. F. Harris: Int. Mater. Rev. **49** (2004) 31.
2) M. Sarikaya and I. A. Aksay: *Biomimetics: Design and Processing of Materials* (AIP, New York, 1995).
3) H. J. Gao, B. H. Ji, I. L. Jager, E. Artz, and P. Fratzl: Proc. Natl. Acad. Sci. U.S.A. **100** (2003) 5597.
4) J. D. Currey: Proc. R. Soc. London, Ser. B **196** (1977) 443.
5) A. P. Jackson, J. F. V. Vincent, and R. M. Turner: Proc. R. Soc. London, Ser. B **234** (1988) 415.
6) J. D. Currey: *Bones: Structure and Mechanics* (Princeton University Press, Princeton, NJ, 2002).
7) L. J. Gibson and M. F. Ashby: *Cellular Solids—Structure and Properties* (Pergamon Press, New York, 1988).
8) L. J. Gibson: J. Biomech. **38** (2005) 377.
9) Y. Shiina, Y. Hamamoto, and K. Okumura: Europhys. Lett. **76** (2006) 588.
10) A. Fazekas, R. Dendievel, L. Salve, and Y. Brechet: Int. J. Mech. Sci. **44** (2002) 2047.
11) S. Choi and B. V. Sankar: Int. J. Solids Struct. **42** (2005) 1797.
12) D. R. Katti, K. S. Katti, J. M. Sopp, and M. Sarikaya: Comput. Theor. Polym. Sci. **11** (2001) 397.
13) C. Hellmich, C. Kober, and B. Erdmann: Ann. Biomed. Eng. **36** (2008) 108.
14) Y. S. Song and J. R. Youn: Polymer **47** (2006) 1741.
15) T. L. Anderson: *Fracture Mechanics* (CRC Press, Boca Raton, FL, 1995) 2nd ed.
16) C. E. Inglis: Trans. Inst. Naval Archit. **55** (1913) 219.
17) A. A. Griffith: Philos. Trans. R. Soc. London, Ser. A **221** (1921) 163.
18) K. Okumura and P.-G. de Gennes: Eur. Phys. J. E **4** (2001) 121; K. Okumura: J. Phys.: Condens. Matter **17** (2005) S2879.
19) Y. Huang and A. J. Kinloch: Polymer **33** (1992) 1330.
20) J. W. Hutchinson: J. Mech. Phys. Solid **16** (1968) 13.
21) J. R. Rice and G. F. J. Rosengren: J. Mech. Phys. Solid **16** (1968) 1.
22) K. Okumura: Europhys. Lett. **67** (2004) 470.
23) S. Nakagawa and K. Okumura: J. Phys. Soc. Jpn. **76** (2007) 114801.
24) G. R. Irwin: in Handbuch der Physik (Springer, Berlin, 1958) Vol. 6, p. 557.
25) E. Orowan: Rep. Prog. Phys. **12** (1949) 185.